

Substrate-induced strain and its effect in CrO 2 thin films

M. Pathak, H. Sato, X. Zhang, K. B. Chetry, D. Mazumdar, P. LeClair, and A. Gupta

Citation: *Journal of Applied Physics* **108**, 053713 (2010); doi: 10.1063/1.3475993

View online: <http://dx.doi.org/10.1063/1.3475993>

View Table of Contents: <http://scitation.aip.org/content/aip/journal/jap/108/5?ver=pdfcov>

Published by the [AIP Publishing](#)

Articles you may be interested in

Strain effect caused by substrates on phase separation and transport properties in Pr_{0.7}(Ca_{0.8}Sr_{0.2})_{0.3}MnO₃ thin films

J. Appl. Phys. **111**, 07D721 (2012); 10.1063/1.3678297

Enhanced magnetization of Cu Cr₂O₄ thin films by substrate-induced strain

J. Appl. Phys. **105**, 07A905 (2009); 10.1063/1.3058612

Impact of yttrium on structure and mechanical properties of Cr–Al–N thin films

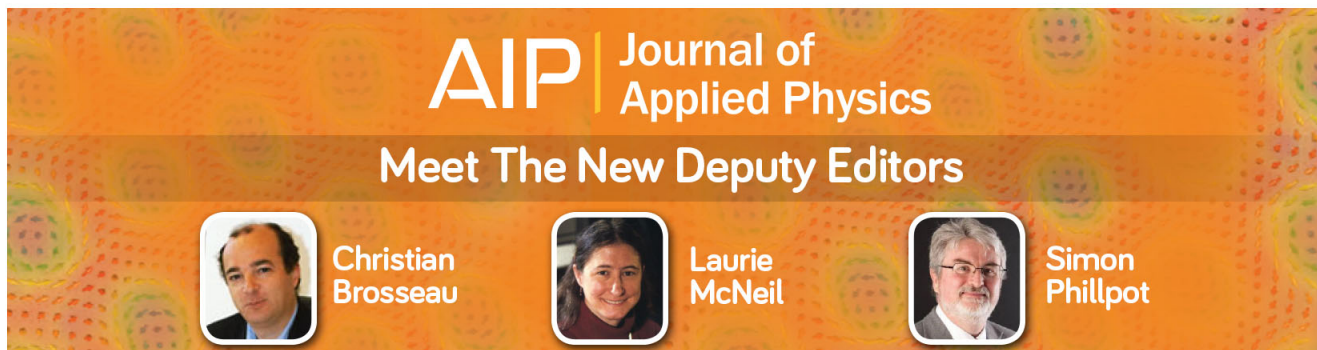
J. Vac. Sci. Technol. A **25**, 1336 (2007); 10.1116/1.2753842

Microstructure and nanohardness properties of Zr–Al–N and Zr–Cr–N thin films

J. Vac. Sci. Technol. A **23**, 593 (2005); 10.1116/1.1924579



Strain effects in thin films of CrO₂ on rutile and sapphire substrates

J. Appl. Phys. **89**, 7696 (2001); 10.1063/1.1362657



AIP | Journal of Applied Physics

Meet The New Deputy Editors

	Christian Brosseau		Laurie McNeil		Simon Phillpot
-------------------------------------------------------------------------------------	---------------------------	-------------------------------------------------------------------------------------	----------------------	---------------------------------------------------------------------------------------	-----------------------

Substrate-induced strain and its effect in CrO₂ thin filmsM. Pathak^{1,2,a)} H. Sato,² X. Zhang,^{2,3} K. B. Chetry,^{1,2} D. Mazumdar,² P. LeClair,^{1,2} and A. Gupta^{2,3,4}¹*Department of Physics and Astronomy, University of Alabama, Tuscaloosa, Alabama 35487, USA*²*MINT Center, University of Alabama, Tuscaloosa, Alabama 35487, USA*³*Department of Chemistry, University of Alabama, Tuscaloosa, Alabama 35487, USA*⁴*Department of Chemical and Biological Engineering, University of Alabama, Tuscaloosa, Alabama 35487, USA*

(Received 13 April 2010; accepted 13 July 2010; published online 9 September 2010)

We report a study of substrate-induced strain and its effect in (100) and (110) CrO₂ thin films deposited on TiO₂ substrates of respective orientations. While the (110) CrO₂ films grow essentially strain-free, the (100) CrO₂ films were found to be strained in all lattice directions—out of plane direction was compressively strained while in-plane directions were under tensile strain. Crystal lattice parameters were determined in strained (100) and strain-free (110) CrO₂ films together with the amount of strain in the three lattice directions. We found substrate-induced strain to significantly affect the magnetic moment in the (100) CrO₂ films at room temperature—reducing the magnetic moment with increasing strain in the (100) films while strain-free (110) CrO₂ thin films have higher moments for all thicknesses. Qualitative macroscopic conductance behavior in the strained (100) and strain-free (110) CrO₂ films were found to be comparable for temperatures in the range of 5–400 K, showing similar behavior at low temperature as well as near T_c. © 2010 American Institute of Physics. [doi:10.1063/1.3475993]

I. INTRODUCTION

CrO₂ has a band gap in its minority density of states around Fermi level¹ making it an example of half-metallic ferromagnet. Being a half-metallic ferromagnetic material, CrO₂ stands as an ideal candidate for spin electronic devices. Experimentally, CrO₂ shows near 100% spin polarization at low temperatures, and so far the highest among all ferromagnetic materials known so far.^{2–4} Therefore, very large tunnel or giant magnetoresistance should, in principle, be obtained in a CrO₂ based device.⁵ CrO₂ can also be used in Josephson junctions, as demonstrated by Keizer *et al.*,⁶ exhibiting a spin valve effect and provides evidence of triplet superconductivity. In addition to its half-metallicity, other interesting properties of CrO₂ thin films are its selective area growth⁷ and magnetic anisotropy controllable by substrate-induced strain.⁸ Further, CrO₂ has a Curie temperature of ~395 K, making near-room temperature plausible. All these properties make CrO₂ a fascinating material of great interest and a promising candidate for spin electronic applications.

Although CrO₂ has all these exciting properties, synthesis of CrO₂ has been challenging, as it is a metastable oxide of chromium. However, high quality CrO₂ films can be grown on TiO₂,⁹ as well as on (0001) Al₂O₃ (Ref. 10) substrates, using an atmospheric pressure two-zone furnace in chemical vapor deposition (CVD), as first described by Ishibashi *et al.*¹¹ CrO₂ and TiO₂ are known to adopt the tetragonal rutile structure in bulk, with lattice parameters $a=b=4.421$ Å, $c=2.916$ Å for CrO₂, and $a=b=4.593$ Å and $c=2.959$ Å for TiO₂. This gives rise to lattice mismatch of 3.75% along (100), (010), (110), and ($\bar{1}10$) directions, and

1.45% along (001) direction between CrO₂ and TiO₂. As a result of this lattice mismatch, substrate-induced strain is expected in CrO₂ films deposited on TiO₂ substrates with the degree of strain varying with growth orientation. CrO₂ films of (100) and (110) orientations were found to grow epitaxially on TiO₂ substrates of their respective orientations. We find (100) films exhibit significant substrate-induced strain, while (110) oriented films do not—attributed to different growth modes followed by (100) and (110) CrO₂ films grown on TiO₂ substrates of respective orientations.⁹ (100) CrO₂ films grow in layer by layer mode on (100) TiO₂ substrate and are strained while (110) CrO₂ films grow in island mode on (110) TiO₂ substrates and are relaxed. Although the reason for strain in the films has been narrowed down to different growth modes of (100) and (110) CrO₂ films, the origin of different growth modes is not very clearly understood. It can be speculated that the origin of different growth modes lies in the surface energy difference between the substrate and the film of respective orientations.¹² Regarding the effect of substrate-induced strain, it is already known that the magnetic properties of (100) CrO₂ films depend on the substrate-induced strain⁸ however; the variation of strain itself in these films has not been very well investigated, in contrast to other oxide films. For example, substrate-induced strain in BiFeO₃ films has been quite thoroughly investigated, and ferroelectric properties in these films are known to change with substrate-induced strain.¹³ In this study, we report a detailed investigation of substrate-induced strain in epitaxial (100) and (110) CrO₂ films as a function of film thickness(es) and its consequences for films' magnetic and transport properties.

a)Electronic mail: mpathak@mint.ua.edu.

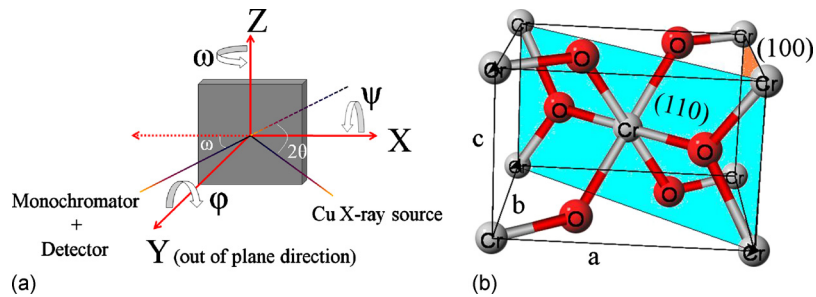


FIG. 1. (Color online) (a) Schematic of the sample geometry for XRD in the Philips X'Pert system. Coordinate axes and rotation about each of them are shown. Here X, Y, and Z are the (010), (100), and (001) directions in case of (100) CrO_2 films, while in case of (110) CrO_2 films, these directions are $(\bar{1}10)$, (110), and (001), respectively. Offsets in φ , ψ , and ω angles are cleared before a $(2\theta-\omega)$ scan. (b) Schematic of CrO_2 unit cell with principal axes and (100) and (110) planes.

II. EXPERIMENTAL DETAILS

We deposited CrO_2 films of (100) and (110) orientations on the respective TiO_2 substrates using a previously reported atmospheric CVD method.^{9,11} For our study, we considered CrO_2 films of thicknesses 25, 45, and 100 nm for both (100) and (110) orientations with a view to investigate the thickness dependence of strain and its influence on other film properties. Substrate-induced strain was investigated and quantified along the a , b , and c axes [i.e., the (100), (010), and (001) directions], respectively, using x-ray diffraction (XRD) performed with a Phillips X'Pert diffractometer at room temperature. The sample geometry for XRD is shown in Fig. 1(a). For both (100) and (110) samples, the (001) direction, i.e., the c -axis in the films is oriented along the z -direction in the sample geometry which is an in-plane direction in both (100) and (110) CrO_2 films. The out of plane directions (y) for (100) and (110) CrO_2 films are basically the respective film growth orientations. The other in-plane directions are the (010) (i.e., b) and $(\bar{1}10)$ directions in case of (100) and (110) CrO_2 films, respectively.

In all our CrO_2 films, the temperature dependence of the magnetic moment was also investigated using a Quantum Design superconducting quantum interference device (SQUID) from 10 to 350 K. The effect of substrate-induced strain on the magnetic moment of the films was determined. We observed the magnetic moment of (100) CrO_2 films to scale with the substrate-induced strain, i.e., lower moment was observed for more significantly strained films. To study how the conductance mechanism might be affected, we measured film resistivity on selectively grown (100) and (110) CrO_2 films on TiO_2 substrates of respective orientations in a

Quantum Design physical property measurement system from 5 to 400 K. We observed similar behavior in both types of films both at low temperature as well as near T_c .

III. RESULTS AND DISCUSSION

Despite the significant lattice mismatch between CrO_2 and TiO_2 , CrO_2 films grow epitaxially on TiO_2 substrates. We can determine the out of plane lattice parameter in an epitaxial CrO_2 film performing a $(2\theta-\omega)$ scan using Bragg's law for XRD: $2d \sin \theta = n\lambda$ ($\lambda = 1.541 \text{ \AA}$ for our Cu x-ray source). To observe diffraction from a desired off axis plane, samples are tilted in required φ , ψ , and 2θ angles. Tilting the samples with ψ , φ , and 2θ angles is basically a rotation of the sample about the x , y , and z axes, respectively, as shown in Fig. 1. These tiltings reduce the diffraction intensities but film peak positions can easily be identified. Figures 2 and 3 show off axis $(2\theta-\omega)$ scans observed on (100) and (110) films, respectively. As seen in Fig. 2, 2θ diffraction positions in the (100) CrO_2 films from (110) and (011) off axis planes for all three film thicknesses are significantly shifted from the bulk CrO_2 diffraction position (the vertical dashed lines), a result of substrate-induced strain along these directions. However, in case of (110) CrO_2 films, 2θ diffraction positions from (200) and (020) off axis planes align perfectly with that in bulk CrO_2 (vertical dashed lines). This suggests the surprising absence of any substrate-induced strain in these directions in (110) CrO_2 films.

To determine the lattice constants, namely a , b , and c in the CrO_2 films, we employed Cohen's method for a tetragonal system, described in references.¹⁴⁻¹⁶ Random errors are reduced in this method due to the least-square approach and

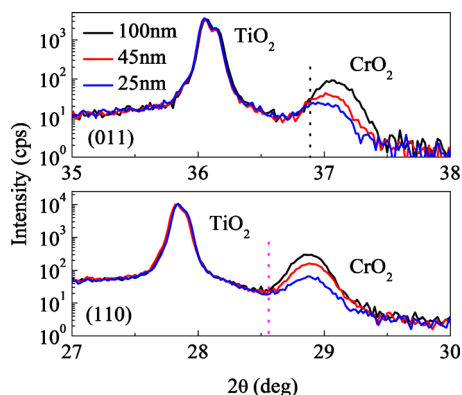


FIG. 2. (Color online) Diffraction from (011) and (110) planes in (100) CrO_2 films of different thickness. Dotted lines represent the bulk 2θ positions.

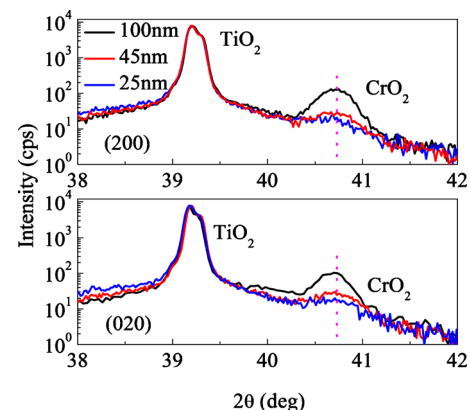


FIG. 3. (Color online) Diffraction from (200) and (020) planes in (110) CrO_2 films of different thicknesses. Dotted lines represent the bulk 2θ positions.

TABLE I. Diffraction angles from different planes of (100) and (110) CrO₂ films of three different thicknesses are listed. Diffraction angles from one plane in (110) CrO₂ films were found to be same for the three different film thicknesses. The angles have an accuracy of $\pm 0.04^\circ$.

CrO ₂ (100)	2θ (°)			CrO ₂ (110)	2θ (°)
	25 nm	45 nm	100 nm		25, 45, 100 nm
(020)	41.30	41.21	41.14	(110)	28.52
(040)	89.70	89.45	89.21	(200)	40.70
(101)	36.65	37.02	37.07	(020)	40.70
(1 $\bar{1}$ 0)	28.37	28.88	28.78	(211)	56.16
(2 $\bar{1}$ 1)	56.39	56.38	56.38	(121)	51.16

the application of appropriate error function reduces possible systematic errors. According to this method, it is required to evaluate the constants A , B , C , and D in the following Eq. (1) below and it is achieved by obtaining diffraction angles (2θ) for different planes:

$$\sin^2 \theta = Ah^2 + Bk^2 + Cl^2 + D\delta, \quad \text{with}$$

$$\delta = 10 \sin^2 2\theta \left(\frac{1}{\sin \theta} + \frac{1}{\theta} \right). \quad (1)$$

Here $A = \lambda^2/4a^2$, $B = \lambda^2/4b^2$, and $C = \lambda^2/4c^2$. (h, k, l) are Miller indices of the relevant plane and the error function is δ . Diffraction positions (2θ) of the planes considered for Cohen's method are shown in Table I. Using the values from Table I in Eq. (1), the lattice constants and resulting strain in these lattice directions were calculated. Lattice constants and unit cell volumes as a function of film thickness are plotted in Fig. 5. We observed compressive strain along the out-of-plane, b direction in (100) CrO₂ films and the thinnest sample (25 nm) has the highest compressive strain of -1.15% ($b = 4.368$ Å). We found that the compressive strain decreased with increasing (100) CrO₂ film thickness—about -0.9% in 45 nm ($b = 4.382$ Å) and -0.6% in 100 nm film ($b = 4.396$ Å).

Tensile strain was observed along the c and a directions in the (100) CrO₂ films, with its magnitude decreasing with increasing (100) film thickness. In 25 nm (100) films, strain along the a direction was 1.8% ($a = 4.500$ Å) and it decreased to 1.56% ($a = 4.492$ Å) and 1.42% ($a = 4.484$ Å) in 45 nm and 100 nm films, respectively. Strain in the c direction was found to be smaller than the strain along a and b directions in the (100) CrO₂ films. In the c direction, 25 nm (100) film had strain of 0.6% ($c = 2.934$ Å) while 45 nm and 100 nm (100) films had strain of 0.54% ($c = 2.932$ Å) and 0.15% ($c = 2.920$ Å), respectively. This indicates that overall the (100) CrO₂ unit cell is more distorted along the in-plane direction a . Therefore, as a result of substrate-induced strain,

the unit cell in a (100) CrO₂ film is compressed in the b direction and consequently expands in the c and a directions leading to an overall tetragonal distortion. Considering a tetragonal unit cell for this strained (100) CrO₂ film, the calculated unit cell volume was found to be slightly larger than the bulk CrO₂ unit cell volume, decreasing toward the bulk value with increasing film thickness.

Overall, the thinnest (100) CrO₂ sample (25 nm) is most significantly strained in all three directions and lattice parameters and unit cell volume converge toward bulk values by ~ 100 nm, indicating that the films are relaxing with increasing thickness. This strained unit cell can be expected to strongly affect the magnetic properties in particular since the exchange and the magnetic moment are very sensitive to the lattice parameters. On the other hand, lattice constants in (110) CrO₂ films for all thicknesses were found to be within ± 0.01 Å of bulk CrO₂ lattice parameters in all three directions and as a result, the (110) CrO₂ unit cell maintained essentially its bulk unit cell volume for all thicknesses and hence little impact on magnetic properties is expected. Calculated TiO₂ substrate lattice parameters were within ± 0.002 Å of bulk TiO₂, demonstrating high quality of the substrates used for film deposition.

Another way of looking at the strain in thin films and film domain structures is reciprocal space mapping (RSM) of lattice plane(s). In Fig. 4, RSM of (031) and (130) planes in (100) CrO₂ film confirms that the film is strained when compared with RSM of the same plane of the (100) TiO₂ substrate, as the CrO₂ intensity region is displaced from the TiO₂ 2θ direction. However, a RSM of the (130) plane in a (110) CrO₂ film on (110) TiO₂ substrate did not show any substrate-induced strain. This RSM image confirms the relaxed growth of (110) films and strained growth of (100) films on respective TiO₂ substrates.⁹ Also, the RSMs indicate single domain evolution of the films as only single significant intensity region in the films could be observed within the scan range. Lattice constants in (100) CrO₂ films were

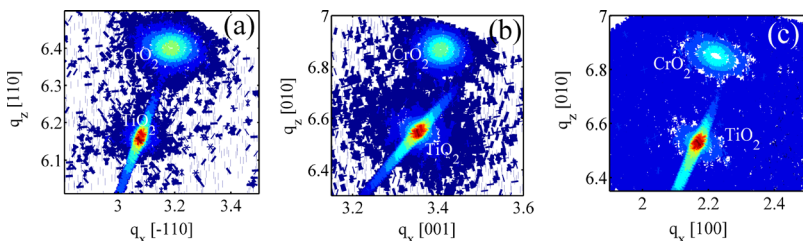


FIG. 4. (Color online) (a) RSM of (130) plane in 45 nm (110) film. [(b) and (c)] RSM of (031) and (130) planes in 45 nm (100) CrO₂ film, respectively. Because of the much smaller thickness of films than the substrates, film intensities are much lower than in substrate region. Strong background in (c) is because of a lower signal to noise ratio in the scans. Here, q_x and q_z represents the horizontal and vertical projections (in per nanometer), respectively, of RSM plane direction.

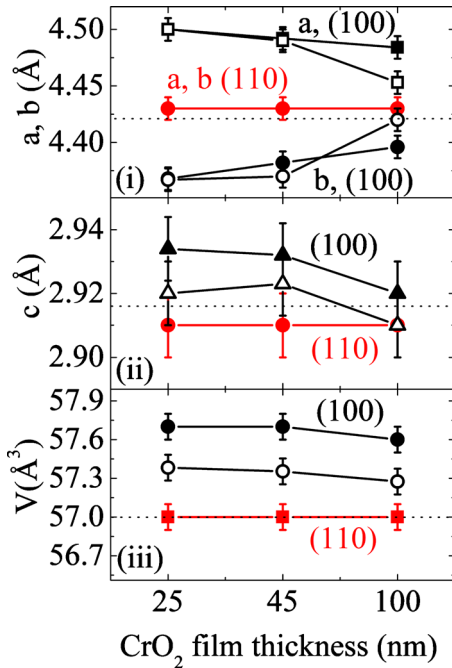


FIG. 5. (Color online) (i) Lattice constants a and b of (100) and (110) CrO_2 films for different thicknesses. (ii) Lattice constant c against thickness. (iii) Unit cell volume against thickness. Open symbols indicate the respective values calculated from RSM of (100) CrO_2 films. Errors in determining lattice constants and unit cell volumes are estimated at 2%–3% of the reported values. The dotted lines in (i), (ii), and (iii) show the respective values of the parameters in bulk CrO_2 .

evaluated from the projections of the center of film intensity on the axes. If q_x and q_z are the projections on the respective axes, from the projections of (031) plane we have $c=1/q_x$ and $b=3/q_z$, and in case of the (130) plane we have $a=1/q_x$ and $b=3/q_z$. As no projection on c was available in our sample geometry (within the range of angles available) for (110) CrO_2 film, we were not able to determine the lattice constants in (110) CrO_2 films from RSM. Lattice constants in (100) CrO_2 films determined using RSM are plotted in Fig. 5 along with lattice constants determined using Cohen's method. As seen in Fig. 5, lattice constants determined by both RSM and Cohen's method for (100) CrO_2 films are in good agreement, showing a similar trend with thickness, i.e., approaching bulk lattice parameters with increasing film thickness as the substrate-induced strain decreases.

Figure 6 shows the saturation magnetic moment of the (100) and (110) CrO_2 films measured in SQUID magnetometer. A magnetic field of 0.5 T was applied along the easy axis direction of the samples at all temperatures to saturate the magnetization. For all thicknesses studied, (110) films showed higher magnetic moment than (100) films at room temperature (~ 300 K), attributed to the strain-free growth of the (110) CrO_2 films on TiO_2 substrates. Assuming Cr has a spin magnetic moment of $2.0 \mu_B$ at low temperatures (~ 10 K) and neglecting any spin or orbital moment arising from the O^{2-} ions, magnetic moments per Cr atom at 300 K are calculated and reported in Table II. We found the Cr moment in (100) CrO_2 films to decrease with decreasing film thickness while (110) films showed no strong trend. We attribute the decreased moment in (100) films to increase in

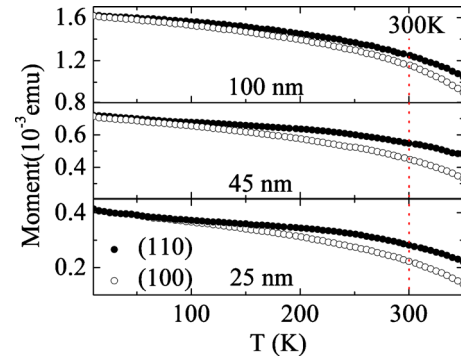


FIG. 6. (Color online) Magnetic moments of (100) and (110) CrO_2 films from 10–350 K measured for three different thicknesses in SQUID. Dashed line is through the moments at 300 K.

substrate-induced strain in the (100) CrO_2 films with decreasing film thickness. This bulk moment analysis on CrO_2 films agrees well with the surface moment analysis on strained and strain-free CrO_2 films previously investigated by magnetic circular dichroism at room temperature.¹⁷

With such a strong alteration of magnetic moment with strain, we investigated possible changes in conductance mechanisms of strained (100) and strain-free (110) CrO_2 films. In this case, we deposited CrO_2 films of both orientations using selective growth method⁷ to define Hall bars of $100 \times 400 \mu\text{m}^2$ patterned on TiO_2 substrates of respective orientations. Both these films had thickness of 70 nm. At that thickness, the (100) CrO_2 film is still significantly strained (they were found to be strained even for thicknesses of more than 200 nm).⁹ Resistivities of our films from 5–400 K are plotted in Fig. 7(a) measured with $100 \mu\text{A}$ current along (001) direction for both films. At all temperatures, resistivities of both films were found to be similar—suggesting the same conductance mechanism in both films and in good agreement with previous reported results on CrO_2 films.^{18–20} Below ~ 35 K, the resistivity approaches a constant value [inset in Fig. 7(b)], and the residual resistivity (ρ_0) of the films and are about $7 \mu\Omega \text{cm}$ and $3 \mu\Omega \text{cm}$ in (100) and (110) films respectively. Lower ρ_0 in (110) films may indicate that the film has less defects than the (100) films, e.g., longer coherence length. We also found higher residual resistivity ratio (RRR), defined as $\rho(300 \text{ K})/\rho_0$ in case of (110) films (RRR ~ 98) than (100) films (RRR ~ 45) as can be observed in Fig. 7(b), indicating that (110) films do exhibit “more metallic” conductance, perhaps consistent with phonon frequencies being altered by substrate-induced strain in (100) CrO_2 films. As no significant temperature dependence of resistivity in the films were observed below ~ 35 K (and hence no T^2 dependence), we can say that there is no significant spin-flip scattering in the films below 35 K. This

TABLE II. CrO_2 moment in the films at 300 K calculated from the SQUID data. Moment values have an accuracy of $\pm 0.05 \mu_B$.

CrO_2 moment (μ_B)	25 nm	45 nm	100 nm
(100)	1.11	1.23	1.43
(110)	1.41	1.51	1.54

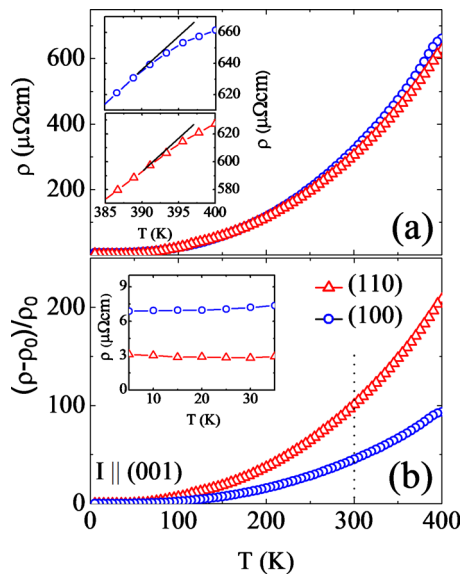


FIG. 7. (Color online) (a) Resistivity plot of (100) and (110) CrO₂ films of thickness 70 nm from 5–400 K. Inset shows the resistivity in the films from 385–400 K. Black lines are drawn to look the slope change more noticeable. (b) $(\rho - \rho_0)/\rho_0$ plot—clearly shows the higher RRR for (110) film. Inset shows the constant resistivity between 5–35 K. The dotted line indicates the room temperature.

is consistent with, though not unambiguous proof of half-metallic behavior, as found.²¹ Resistivity alone does not preclude both films being half-metallic below this temperature. With increasing temperature (~ 100 K), the minority spin channel is expected to contribute to the conductance giving temperature dependence of resistivity as expected for a nonhalf-metallic ferromagnetic material. The insets in Fig. 7(a) show the small but noticeable changes in slopes in the resistivity plots between 390–395 K in both (100) and (110) films. This suggests that the ferromagnetic state is lost in both films between these temperatures.²² It is known that in a ferromagnetic metal, the contribution to resistivity above T_c due to spin disorder is constant, while contribution due to phonon scattering increases as temperature increases,²² and as a result, the slope changes near T_c . The similar changes in slopes in both films imply only a small, if any, change in T_c .¹⁷

IV. CONCLUSION

In summary, we determined the lattice constants and degree of substrate-induced strain along the principal lattice directions in (100) CrO₂ films grown on (100) TiO₂ substrate. Out of plane directions are compressively strained while in-plane directions are in tensile strain in (100) CrO₂

films. Strain along the a direction (100) was found to be more significant than strain along b and c directions, i.e., (010) and (001) directions. (110) CrO₂ films were found to be strain-free in all lattice directions—attributed to relaxed growth of (110) CrO₂ films on (110) TiO₂ substrates. We also observed that substrate-induced strain significantly reduces the magnetic moment in (100) CrO₂ films at room temperature. In spite of the substrate-induced strain in (100) CrO₂ films, similar transport behavior was observed in both (100) and (110) CrO₂ films—both at low temperatures as well as near T_c .

ACKNOWLEDGMENTS

We thank CrySTec, Berlin, Germany for providing very high quality TiO₂ substrates. This work has been supported by funding from NSF under Grant No. DMR-0706280.

- ¹M. A. Korotin, V. I. Anisimov, D. I. Khomskii, and G. A. Sawatzky, *Phys. Rev. Lett.* **80**, 4305 (1998).
- ²J. Parker, S. Watts, P. Ivanov, and P. Xiong, *Phys. Rev. Lett.* **88**, 196601 (2002).
- ³A. Anguelouch, A. Gupta, G. Xiao, D. W. Abraham, Y. Ji, S. Ingvarsson, and C. L. Chein, *Phys. Rev. B* **64**, 180408(R) (2001).
- ⁴K. A. Yates, W. R. Branford, F. Magnus, Y. Miyoshi, B. Morris, L. F. Cohen, P. M. Sousa, O. Konde, and A. J. Silvestre, *Appl. Phys. Lett.* **91**, 172504 (2007).
- ⁵M. Julliere, *Phys. Rep.* **54A**, 225 (1975).
- ⁶R. S. Keizer, S. T. B. Geonnenwein, T. M. Klapwijk, G. Miao, G. Xiao, and A. Gupta, *Nature (London)* **439**, 825 (2006).
- ⁷A. Gupta, X. W. Li, S. Guha, and G. Xiao, *Appl. Phys. Lett.* **75**, 2996 (1999).
- ⁸G. Miao, G. Xiao, and A. Gupta, *Phys. Rev. B* **71**, 094418 (2005).
- ⁹K. B. Chetry, M. Pathak, P. LeClair, and A. Gupta, *J. Appl. Phys.* **105**, 083925 (2009).
- ¹⁰P. M. Sousa, S. A. Dias, O. Konde, A. J. Silvestre, W. R. Branford, B. Morris, K. A. Yates, and L. F. Cohen, *Chem. Vap. Deposition* **13**, 537 (2007).
- ¹¹S. Ishibashi, T. Namikawa, and M. Satou, *Mater. Res. Bull.* **14**, 51 (1979).
- ¹²K. B. Chetry, H. Sims, W. H. Butler, and A. Gupta, “Surface energies, interface energies, and growth modes for CrO₂ films” (unpublished).
- ¹³S. Nakashima, D. Ricinchi, J. M. Park, T. Kanashima, H. Fujisawa, M. Shimizu, and M. Okuyama, *J. Appl. Phys.* **105**, 061617 (2009).
- ¹⁴M. U. Cohen, *Rev. Sci. Instrum.* **6**, 68 (1935).
- ¹⁵J. I. Langford, *J. Appl. Crystallogr.* **6**, 190 (1973).
- ¹⁶B. D. Cullity and S. R. Stock, *Elements of X-Ray Diffraction*, 3rd ed. (Prentice Hall, Upper Saddle River, New Jersey, 2001), pp. 376–381.
- ¹⁷M. Pathak, H. Sims, K. B. Chetry, D. Mazumdar, P. R. LeClair, G. J. Mankey, W. H. Butler, and A. Gupta, *Phys. Rev. B* **80**, 212405 (2009).
- ¹⁸A. Gupta, X. W. Li, and G. Xiao, *J. Appl. Phys.* **87**, 6073 (2000).
- ¹⁹A. Barry, J. M. D. Coey, L. Ranno, and K. Ounadjela, *J. Appl. Phys.* **83**, 7166 (1998).
- ²⁰K. Suzuki and P. M. Tedrow, *Phys. Rev. B* **58**, 11597 (1998).
- ²¹C. G. F. Blum, C. A. Jenkins, J. Barth, C. Felser, S. Wurmehl, G. Friemel, C. Hess, G. Behr, B. Buchner, A. Reller, S. Reigg, S. G. Ebbinghaus, T. Ellis, P. J. Jacobs, J. T. Kohlhepp, and H. J. M. Swagten, *Appl. Phys. Lett.* **95**, 161903 (2009).
- ²²M. J. Otto, R. A. M. van Woerden, P. J. van der Valk, J. Wijngaard, C. F. van Bruggen, and C. Haas, *J. Phys.: Condens. Matter* **1**, 2351 (1989).